Equivalence Principle parity violation tests

Alan M. Schwartz
xenophage@gmail.com
28 November 2008

Abstract
Gravitation is parity symmetric or antisymmetric. Mass distribution parity divergence varies from $\chi = 0$ (achiral) to $\chi = 1$ (perfect). A parity Eötvös experiment contrasts chemically and macroscopically identical enantiomorphic space groups $P3_121$ and $P3_221$ α-quartz single crystal test masses. A parity calorimetry experiment contrasts $P3_121$ and $P3_221$ benzil single crystals' enthalpies of fusion. A model chiral vacuum detection is calculated. It is shown that Equivalence Principle parity violation is deeply testable given common materials and instrumentation.

PACS numbers: 04.80.Cc, 11.30.Er

I. INTRODUCTION

Galileo's 1638 universality of free fall, Newton's 1687 invariant proportionality of mass and weight, and Einstein's 1907 elevator postulate the weak Equivalence Principle (EP): All local centers of mass vacuum free fall along identical minimum action trajectories independent of composition or internal structure. Gravitational (m_g) and inertial (m_i) masses are indistinguishable. General relativity (GR) is exact within observational uncertainty.

Observables are free fall inert. All atoms are anonymous unit masses, chemical bonding is invisible. Polarized electron spin and orbital angular momentum test masses validate the EP[1]. GR describes 1.74 solar-mass pulsar PSR J1903+0327 in a 95.17-day 0.437-eccentricity orbit with its 1.05 solar-mass companion: 27% vs. 1.4×10^{-4}% gravitational binding energy, 1.8×10^{11} vs. ~30 surface gees, 2×10^8 gauss vs. ~5 gauss magnetic field, neutrons and exotica vs. protons and electrons; pulsar equatorial spin >11% lightspeed[2].

La Coupe du Roi[3] gaplessly dissects a symmetric form into homochiral pieces. Ashtekar and thereafter[4] analogously divided GR into a chiral pair. Teleparallel gravitation is translation group gauge theory with EP ignored. GR obtains if EP = true. EP = false torsion resembles Lorentz force in electrodynamics[5]. Both are chiral: Mirror images (one coordinate axis inverted) are not superposable. Parity inverts all three coordinate axes.

Torsion vacuum is a left foot. Socks (achiral mass distributions) and left shoes similarly insert. Their free fall trajectories coincide. Right shoes insert differently. Their free fall trajectories diverge. Opposite parity atomic mass distributions compel EP parity violation. The massless U(1) sector, lacking configuration, is unaffected.

Parity-sparing Eötvös experiments test for divergent dynamics, $2|m_g - m_i|/(m_g + m_i)$. Parity-destroying calorimetry tests, melting left and right shoes into identical achiral socks, observe divergent static insertion energies plus divergent dynamics with overall $|m_g - m_i|c^2$ output amplitude advantage. The EP can empirically fail.

II. SYMMETRIES AND PROPERTIES

True chiral systems exist in two distinct enantiomorphic states interconverted by space inversion but not by time reversal combined with any proper spatial rotation[6]. Chirality is an emergent phenomenon requiring at least four non-coplanar points in 3-space. The ratio of emergent scale to experimental scale is consequential.

EP parity divergence is geometric not compositional or electronic. Optical chirality (the time-reversal even, imaginary part of the complex gyrotropy tensor)) is progressive rotation of the plane of linearly polarized light with passage through a medium. It is an artifact of electronics and interrogation frequency[7]. 2-norbornanone has $[\alpha]_D = 29.8^\circ$ and $\chi = 0.729353$; 2-norbornenone has $[\alpha]_D = 1146.^\circ$ and $\chi = 0.765720$[8]. Silver thiogallate, $AgGaS_2$ with non-polar achiral tetragonal space group I-42d, has 522°/millimeter optical rotation along [100] at 497.4 nm[9]. α-Quartz in enantiomorphic space groups $P3_121$ and $P3_221$ has no measurable optical chirality 56.16° from crystallographic [0001][10]. Identical homochiral units cancel in *La Coupe du Roi*. χ for the entire atomic mass distribution is required.

Internal symmetries' coupled observables transform fields amongst themselves leaving translation and rotation unchanged. A local gauge transformation always exists to make the local gauge-field vanish. Two vector potentials differing only by a gauge transformation give the same field. EP tests opposing internal symmetries' observables are first order default nulls: baryon number, charge conjugation, electric charge, lepton number, hypercharge, weak hypercharge, electroweak force, isospin, weak isospin, G-parity, R-parity, quark color, quark flavor.

Parity is the only discrete external symmetry with no continuous approximation. It is excluded from Taylor expansions, smooth Lie groups, and Noether's theorem. Invariance of a linear differential operator under a discrete symmetry requires a partial differential equation invariant under reflection to possess solutions that are also invariant. If **G** is the Hermitian generator of nontrivial unitary operator **U** (e.g., parity), then if **U** commutes with Hamiltonian **H**, then so does **G**: [**H**,**G**] = 0. If **U** commutes with **H** it is a symmetry and a conserved quantity. Any system initially in an eigenstate of **U** evolves over time to other eigenstates with the same eigenvalue. Parity external symmetry-property coupling is a unique.

Resolved enantiomers in prior enthalpy of racemization, solution, or combustion studies did not meet parity divergence geometric criteria. Astronomic resolved parity bodies do not exist. L-amino acids (protein) and D-sugars (cellulose) cancel in a parity Nordtvedt effect. EP parity violation below 10^{-12} difference/average does not contradict any prior observation in any venue at any scale[11].

III. PARITY EÖTVÖS AND CALORIMETRY EP TESTS

Geocenter orbital acceleration varies from 0.6133 cm/sec^2 03 January perihelion to 0.5737 cm/sec^2 05 July aphelion, averaging 0.5930 cm/sec^2 at one astronomical unit. Given World Geodetic System 1984, 44.95º latitude affords maximum 1.693 cm/sec^2 horizontal component of Earth's spin at sea level. Small imposed accelerations demand large contrasted property concentration and divergence for detectable non-zero EP violation.

Composition test mass properties are small fractions of total mass. Their difference is no more than <0.2 mass-% net divergence. Essentially 100% of extremal parity test mass is actively divergent: nuclear mass arguably plus position-averaged non-valence electrons' mass, presented in Table I.

TABLE I. Single body (active mass)/(rest mass).

Property	Fraction of rest mass
enantiomorphic crystal	99.9726% quartz
geometric parity divergence[a]	99.9713% benzil
Nuclear binding energy (low Z)	0.76% ^{4}He
Neutron versus proton mass	0.14%
Electrostatic nuclear repulsion	0.06%
Electron mass	0.03%
Unpaired spin mass	0.005% ^{55}Mn[b]
Nuclear antiparticle exchange	0.00001%
Weak Force interactions	0.0000001%
Gravitational binding energy	0.000000046% Earth[c]
	0.0000000019% moon

[a] (nuclear mass)/(atomic mass) weighted for isotopic abundance
[b] Modeled as the aligned undecatiplet
[c] Iron core rather than homogeneous body

An Eötvös torsion pendulum is the EP test gold standard. A symmetric ~6 cm diameter rotor is vertically suspended from a meter of minimal diameter fiber. It holds two balanced sets of 180°-opposed test masses totaling about 40 grams. EP violation exerts periodic torque. Composition tests null to 5×10^{-14} difference/average[12].

A parity Eötvös experiment contrasts space group $P3_121$ versus $P3_221$ α-quartz solid single crystal spheres (no direction bias). Hemiparity Eötvös experiments contrast α-quartz and amorphous fused silica test masses. Fused silica's smaller density, 2.649 and 2.203 g/cm^3 respectively, requires 0.878% undersized radii with total mass deficit restored by 19.3 g/cm^3 gold plating to full radius. Non-zero net output falsifies the EP.

Benzil is an achiral flat molecule molten, gas phase, or in solution. Solid state lattice forces twist the molecules and align them into homochiral helices spanning a crystal's c-axis. They parallel stack into a triangular lattice, space group $P3_121$ or $P3_221$ exclusively. Crystal melts are achiral and indistinguishable.

Two horizontally abutted differential scanning calorimeters' sample ports define a north-south line. Each holds a ~3 mm diameter ~17 mg benzil solid single crystal sphere, sample carriers sealed against sublimation: consistently one in space group $P3_121$, the other in $P3_221$. ΔH_{fusion} are simultaneously run. New crystals run at half-hour intervals from 0500 hrs to 1900 hrs inclusive local time. If $\Delta\Delta H_{fusion} > 0$ within experimental error repeat the run the next day with east-west alignment. $\Delta\Delta H_{fusion}$ will have a six hour phase shift on the second day. Controls are ΔH_{fusion} of finely powdered racemic benzil. Non-zero output sums static vacuum insertion parity divergence energy with classical dynamic Eötvös experiment signal as $|m_g - m_i|c^2$. Non-zero net output falsifies the EP.

IV. QUANTITATIVE GEOMETRIC PARITY DIVERGENCE

Invert a thin, pliable, unstretchable left glove into a right glove. A d-dimensional set with $N \geq (d + 2)$ points can continuously transform into its mirror image absent achiral intermediates[13]. A continuous function including extreme opposite values and zero without forced passage through zero during inversion is required.

The International Union of Crystallography defines a crystal as "any solid having an essentially discrete diffraction diagram" including periodic, quasiperiodic, and modulated lattices; incommensurate, misfit, or composite structures, and polytypes. Atom coordinates within a periodic crystal are known given unit cell space group, axis lengths and angles, and unique fractional coordinates of contents.

Principal axes of a body set its center of mass and its N atoms' coordinates. Invert all coordinates' signs to create the opposite parity set. χ is the normalized quantitative parity divergence of the set[14]. χ is globally minimum for all rotations (R) and translations (t) for all correspondences (P) permitted by the colors and/or graph as in Eq. (1):

$$\chi = d[(Min_{\{P,R,t\}}D^2)/4T] \qquad (1)$$

where "d "is the Euclidean dimension, "D^2" is the sum of "N" squared-distances between the set and its inversion for a fixed pairwise correspondence with coincident centers of mass, and "T" is the geometric inertia of the set. χ varies between zero (achiral; superposable inversions) and one (perfect divergence) inclusive. χ is a continuous function of coordinates only - independent of translation, scale, or size (but not aggregation; Section V). One value exists for the set and its parity inversion. QCM software given coordinates calculates χ and diagnostics.

QCM begins by enumerating graph automorphisms in concentric layers of the set starting at its origin. "Direct symmetry index" DSI runs from 0 to 1 inclusive. It is the normalized minimized sum of N squared-distances between the vertices of the d-set and the permuted d-set. DSI > 0 beyond a few contained unit cells disqualifies candidate parity test masses.

"Correspondences" COR integer increases with detected symmetry elements locally and globally. COR is at least 1 (the identity element) with no upper bound. Assigning different atom labels (e.g., SiO_2) does not default assign different graph theory point colors. Lattice chiralities only arising from composition are unsuitable. COR > 1 beyond a few contained unit cells disqualifies candidate parity test masses.

QCM outputs are independent of input file format, atom connectivity, and list ordering. If $\chi \rightarrow 1$ with increasing radius while DSI=0 and COR=1obtain through a few unit cells to ~1200 atoms in QCM, specific code can calculate atom coordinates within successively larger radii, then lattice ball χ values without DSI and COR at ~10^7 atoms/second in a personal computer.

χ given DSI = 0 and COR = 1 is a connection between eigenvalues, special functions, their representation theory with solid angles, and exponentials of fractions of pi at a characteristic scale[15], Eq. (2) emerges.

$$\log(1-\chi) = (-2/3)[\log(\text{atoms})] + \text{intercept} \qquad (2)$$

The intercept is modeled with the smallest solid angle subtended by the vertex angle Φ of a polyhedron (the supplement of its dihedral angle) within a crystallographic screw axis, Eq. (3),

$$\log(1-\chi) = -2[\log(\text{radius, Å})] + [\pi(180-\Phi)/60] - \pi \qquad (3)$$

A crystallographic space group is a group of automorphisms with a bounded fundamental region. Chiral crystal structures (65 Sohncke space groups of 230 3-space periodic space groups) as such are insufficient for constructing parity test masses[16]. Eleven pairs of enantiomorphic space groups in the 65 include three pairs containing both senses of screw axes and five pairs containing 2_1 screw axes (simultaneously left- and right-handed). Space groups $P3_121$ / $P3_221$, $P3_112$ / $P3_212$, and $P3_1$ / $P3_2$ are more robust.

V. REDUCTION TO PRACTICE

EP parity tests require opposed identical composition and macroscopic form test masses such that

1) Essentially 100% of rest mass is active mass.
2) Parity divergence calculation is *ab initio* from relative atom coordinates only.
3) Opposed masses are maximally parity divergent: DSI=0, COR=1, $(1-\chi)>10^{-10}$; $I_x = I_y = I_z$.

$$\sum_i \left(I_{x_i} \times I_{y_i}\right) = \sum_i \left(I_{x_i} \times I_{z_i}\right) = \sum_i \left(I_{y_i} \times I_{z_i}\right) = 0 \qquad (4)$$

Products of moments of inertia $I_{x,y,z}$ are summed over "i" contained atoms[17].

4) A test mass has a sub-nanometer chirality emergent scale gaplessly accumulating in-phase to centimeter dimensions and gram masses (self-similar periodic single crystal).
5) Quality single crystals for test mass fabrication can be grown. ($P3_112$ / $P3_212$ delaminate)
6) χ resists decrease given sparse noise: impurities, vacancies, interstitials, dislocations, mosaicity.
7) Both resolved parities are available absent a ferroelectric phase; allotropy, polymorphism, polytypism, magnetic inclusions, amorphous volumes, disinclinations; electrical (Dauphiné) twinning, and optical (Brazil) twinning.
8) Parity experiments run in unmodified composition apparatus with unchanged protocols.
9) Net output greater than experimental sensitivity is unconstrained by prior observations.
10) Non-zero net output falsifies the EP.

X-ray (scattered by electrons) and neutron (scattered by nuclei) α-quartz diffraction structures are identical within experimental error. Mass has consistent coordinates, listed in Table II.

TABLE II. Coordinates of $P3_221$ α-quartz atoms and nuclei at 298°K

Diffraction method	Unit cell axes, Å a,b	c	Volume, nm^3	Fractional coordinates x/a	y/b	z/c		Smallest helix vertex angle
x-ray [18]	4.9137	5.4047	0.11301	0.4697	0.0000	1/6	**Si**	110.56°
				0.4133	0.2672	0.2855	**O**	
neutron [19]	4.9134	5.4052	0.11301	0.4701	0.0000	1/6	**Si**	110.53°
				0.4136	0.2676	0.2858	**O**	

Inhomogeneity (atom or not atom), unit cell anisotropy (unique c-axis), and dependence of χ upon inertial moments give substantial fluctuations around a uniform trend as test mass radius increases. χ values for increasing radius single crystal spherical balls of α-quartz or benzil[20] give slopes and intercepts consistent with Eq. (2). Pearson correlation is 0.9945 for α-quartz and 0.9880 for benzil.

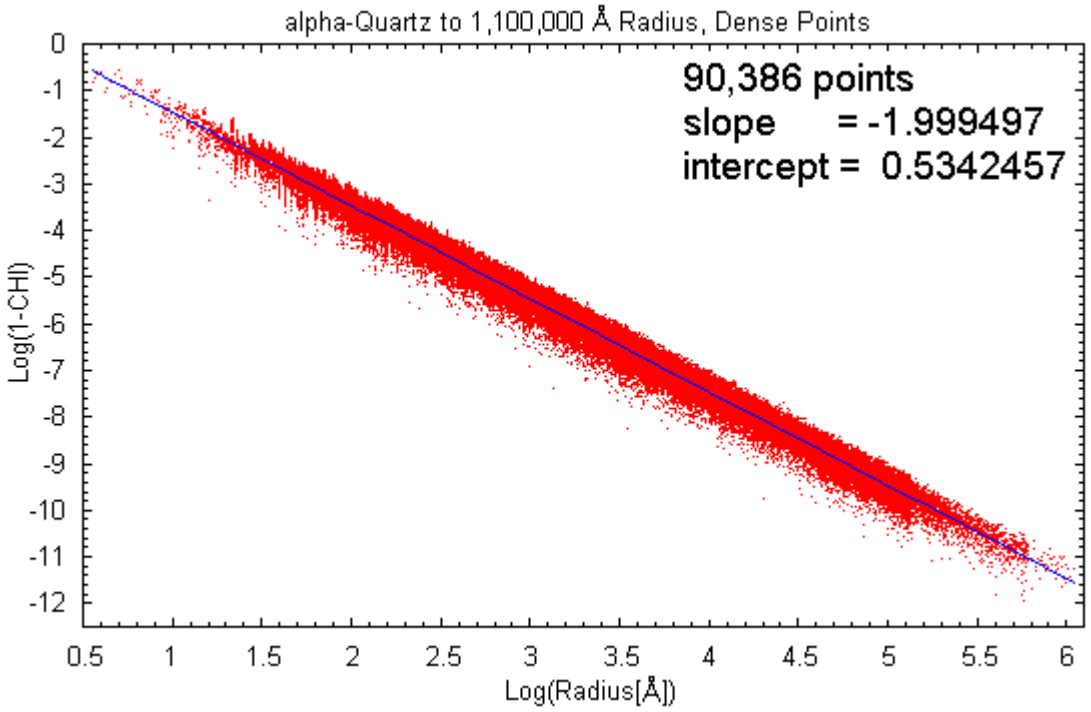

FIG. 1. Approach to χ=1 by α-quartz by radius to 4.44×10^{17} atoms.

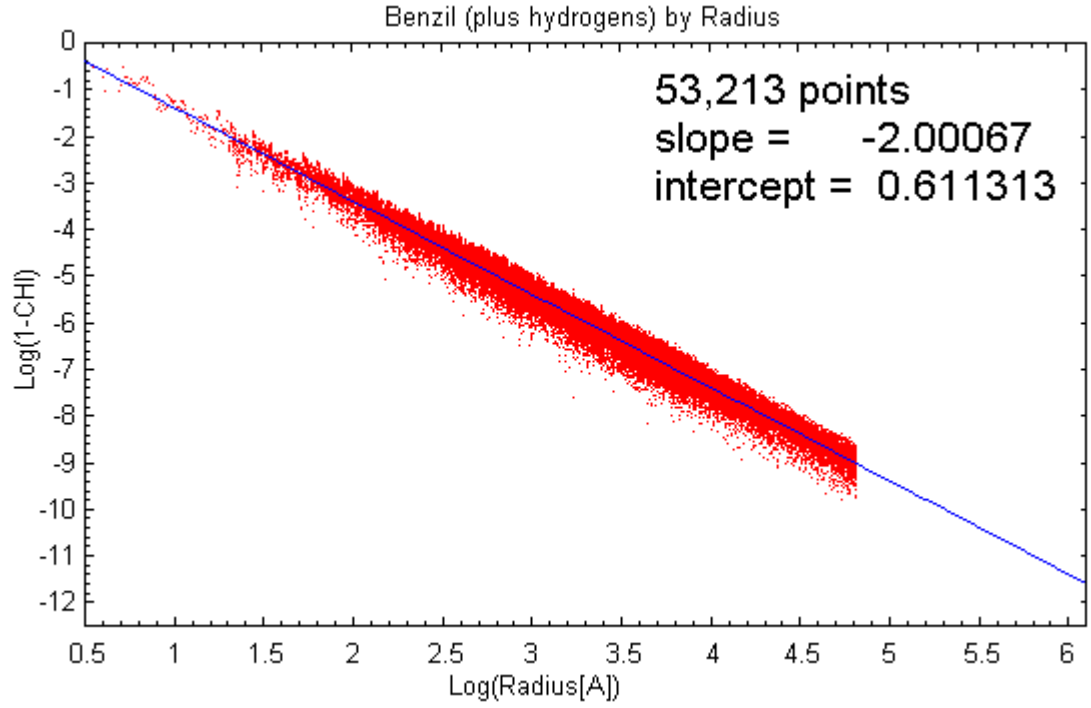

FIG. 2. Approach to χ=1 by benzil by radius to 1.07×10^{14} atoms.

If "R" is radius and "r" is the smallest radius increment that reliably includes more crystal lattice atoms, both in angstroms, then empirically

$$r \approx 10/R^2 \qquad (5)$$

Small radius sampling density is limited by χ change with radius increment. Large radius sampling density is limited by calculation time increasing as $(\text{radius})^2$. Fitted slopes and intercepts rapidly stabilize at high sampling densities, Table III. Parity divergence arising from macroscopic form fails at sub-nanometer scales. α-Quartz SiO_3 chirality emergent scale is within a 0.304 nm diameter sphere. The benzil (C=O)-(C=O) torsion angle is within a 0.313 nm diameter sphere.

TABLE III. Modeled and graphic fits of log(1 - χ) versus log(radius)

Crystal lattice	Lattice volume/atom, nm^3	Smallest vertex angle	Modeled intercept, slope	Graphic intercept, slope	$(1 - \chi)x10^{15}$, diameters 1.5 cm Eötvös	3 mm calorimetry
α-quartz	0.01256	O-Si-O	0.49428	0.53425	0.5548	model
SiO_2		110.56º	-2 exactly	-2.00000	0.6083	graph
benzil	0.01070	(C=O)-(C=O)	0.58643	0.61131	model	17.15
$(C_6H_5CO)_2$		torsion angle 108.80º	-2 exactly	-2.00067	graph	17.96

Classically oppose Be versus Mg (nuclear binding energies)/baryon[21]. Neutron and proton mass equivalents are weighted for magnesium isotopic abundance. A small net difference/average active mass fraction emerges,

p = 938.271998 MeV
n = 939.565330 MeV
Be = 6.462844 MeV/baryon binding energy
Mg = 8.265129 MeV/baryon binding energy
[Mg - Be]/[(17.3202n+16p)/33.3202] = 0.001919

1.5 cm diameter, 4.68 g α-quartz single crystal test masses have $(1 - \chi) = 6x10^{-16}$ with (active mass)/(rest mass) > 0.9997. The parity Eötvös experiment has a 521-fold active mass fraction advantage over composition contrast. 3 mm diameter, 17.7 mg benzil single crystal test masses have $(1 - \chi) = 2x10^{-14}$. Benzil has $\Delta H_{fusion} = 112$ J/g at 95°C in a 0.1% precision differential scanning calorimeter. Given 10^{-13} difference/average Eötvös experiment divergence, parity calorimetry measures difference $|m_g - m_i|c^2$, 8.99 J/g or 8% divergence. Parity calorimetry is 41,000 times more sensitive than a composition Eötvös experiment.

VI. MODELING CHIRAL VACUUM INTERACTION

A direction-unbiased chiral background, opposite parity mass distribution probes, and objective interactions are required. Rigid, uncharged, carbon atom chiral mass distributions were abutted and mm+ energy minimized in HyperChem. Point group **I** (not $\mathbf{I}_h$), $\chi = 1$, giant fullerenes[22] provided interior and exterior chiral vacua. They have six C_5 rotation axes, ten C_3 rotation axes, and fifteen C_2 rotation axes of symmetry. Neutral C_{21} (stripped of 16 hydrogen atoms)[23] is the smallest point group **T** (not $\mathbf{T}_d$ or $\mathbf{T}_h$), $\chi = 1$, rigid probe. It has four C_3 rotation axes and three C_2 rotation axes of symmetry.]

Fullerenes and C_{21} were independently minimized Fullerene larger diameters pass through the centroids of opposite pentagonal faces. Smaller diameters are C_3-axes encircled by three pentagonal faces on each side. C_{21} 4.401688 Å diameters are not co-linear with a bond to the center atom. 3.842750 Å diameters are co-linear with a bond to the center atom. Inverting C_{21} through its center carbon created the opposite parity case, 184.603043 kcal/mole either way. Paired systems were minimized with no imposed constraints. Up to 32,700 iterations of Newton-Raphson block diagonal method were alternated with up to 5000 iterations of Fletcher-Reeves and Polak-Ribière conjugate gradient methods until less than 1 ppm gradient remained or energy values were stable. Table IV lists system values for [*R*]- or [*S*]-C_{21} placed external or internal to fullerenes and allowed to drift to minimum energy separation and orientation. Homochiral and heterochiral interactions within a system were never degenerate. The minimized pairs' atoms' coordinates were then used to calculate gravitational force between each fullerene and probe along their centers of mass line.

TABLE IV. Chiral probes of chiral fullerenes, chemistry

Species	Diameter, Å	Energy, kcal/mole	External, kcal/mole	$\|R - S\|$, cal/mole	Internal, kcal/mole	$\|R - S\|$, cal/mole
C140	10.510002					
	10.438714	250.252945				
[*R*]-C_{21}			429.272308		397.767517	
[*S*]-C_{21}			429.270813	1.495	397.771393	3.876
C260	14.829675					
	14.070113	171.089127				
[*R*]-C_{21}			349.110229		329.561249	
[*S*]-C_{21}			349.112335	2.106	329.561707	0.458
C420	19.299572					
	17.605908	-11.537921				
[*R*]-C_{21}			165.829681		152.796738	
[*S*]-C_{21}			165.827225	2.456	152.798828	2.090
C560	22.550720					
	20.402068	-213.053406				
[*R*]-C_{21}			-36.138103		-47.676041	
[*S*]-C_{21}			-36.143475	5.372	-47.676617	0.207
C980	30.404551					
	26.852409	-892.656372				
[*R*]-C_{21}			-716.276733		-726.759888	
[*S*]-C_{21}			-716.283264	6.531	-726.760010	0.122

Atoms are identical unit masses; G = 1. Species' centers of mass were their atoms' averaged coordinates. Near-field gravitation summed (N + 21)(N + 20)/2 unique paired atoms' force projected on the fullerene-probe centers of mass line. Tables V and VI display chirality-dependent gravitation.

TABLE V. External chiral probes of chiral fullerenes, gravitation

Species	Centers of mass separation, Å	Near-field gravitation	$\|R - S\|$, $x10^4$
C140 [*R*]-C_{21}	9.807581	30.325329	
[*S*]-C_{21}	9.807505	30.327495	21.66
C260 [*R*]-C_{21}	11.646226	39.791141	
[*S*]-C_{21}	11.646276	39.788057	30.84
C420 [*R*]-C_{21}	13.520385	47.417338	
[*S*]-C_{21}	13.520470	47.420889	35.51
C560 [*R*]-C_{21}	14.822984	52.155171	
[*S*]-C_{21}	14.822824	52.163895	87.24
C980 [*R*]-C_{21}	18.051920	60.581705	
[*S*]-C_{21}	18.051704	60.592901	111.96

TABLE VI. Internal chiral probes of chiral fullerenes, gravitation

Species	Centers of mass separation, Å	Near-field gravitation	$\|R - S\|$, $x10^4$
C140 [*R*]-C_{21}	$1.080603x10^{-7}$	$1.808143x10^{-6}$	
[*S*]-C_{21}	$8.240824x10^{-8}$	$1.814732x10^{-6}$	$6.589x10^{-5}$
C260 [*R*]-C_{21}	2.077588	0.0199954	
[*S*]-C_{21}	2.077623	0.0201692	1.738
C420 [*R*]-C_{21}	4.316473	0.277513	
[*S*]-C_{21}	4.316254	0.277131	3.820
C560 [*R*]-C_{21}	5.930397	0.752323	
[*S*]-C_{21}	5.930522	0.752425	1.020

C980 [*R*]-C_{21}	9.832509	2.667019	
[*S*]-C_{21}	9.832498	2.666958	0.610

VII. CONCLUSION

Theories are cast into metric or teleparallel geometries. Equivalence Principle violation tests are proposed using chemically and macroscopically identical, single crystal opposite parity atomic mass distributions: enantiomorphic crystallographic space groups $P3_121$ and $P3_221$ α-quartz (parity Eötvös experiment, parity-sparing) or benzil (parity calorimetry experiment, parity-destroying). Non-null net outputs are consistent with teleparallel theory torsion. They falsify the EP, casting doubt upon metric theory (EP postulated), perturbative string theory (BRST invariance required), and conservation of angular momentum for opposite parity mass distributions (anisotropic vacuum and Noether's theorem). Somebody should look.

ACKNOWLEDGMENTS

Michel Petitjean (geometric theory and QCM), John Osborn (crystallography), John Hooper, Jon Wright (support software). QCM into FastCHI by Matthew Francey; into BigCHI by Anthony J. Lapen and Anne Marie Merritt; into parallelized CHIpir by John E. Scott. χ calculation of SiO_2: Advanced Micro Devices, Inc; John Scott; Zsolt Zsoldos, Anne Marie Merritt, Roy Culley, Ivan Reid.

[1] B. R. Heckel, C. E. Cramer, T. S. Cook, E. G. Adelberger, S. Schlamminger, and U. Schmidt, "New CP-Violation and Preferred-Frame Tests with Polarized Electrons", Phys. Rev. Lett. **97**, 021603 (2006); Rogers C. Ritter, Charles E. Goldblum, Wei-Tou Ni, George T. Gillies, and Clive C. Speake, "Experimental test of equivalence principle with polarized masses", Phys. Rev. D **42,** 977 (1990); Li-Shing Hou, Wei-Tou Ni, and Yu-Chu M. Li , "Test of cosmic spatial isotropy for polarized electrons using a rotatable torsion balance", Phys. Rev. Lett. **90**, 201101 (2003).

[2] D. J. Champion, et al., "An Eccentric Binary Millisecond Pulsar in the Galactic Plane", http://arxiv.org/abs/0805.2396

[3] István Hargittai, Magdolna Hargittai, *Symmetry through the eyes of a chemist,* 2nd Edition (Springer, 1995), pp. 75-78.

[4] S. Mercuri, Phys. Rev. D **73**, 084016 (2006).

[5] R. Aldrovandi, J. G. Pereira, "Gravitation: in search of the missing torsion", http://arxiv.org/abs/0801.4148; R. Aldrovandi, J. G. Pereira, K. H. Vu, "Selected topics in teleparallel gravity", Braz. J. Phys. 34(4a), 1374 (2004). Wei Li, Wei Song, Andrew Strominger, " Chiral Gravity in Three Dimensions" http://arxiv.org/abs/0801.4566; Carlo R. Contaldi, Joao Magueijo, Lee Smolin, "Anomalous CMB polarization and gravitational chirality" http://arxiv.org/abs/0806.3082; Martin Bojowald, Rupam Das, "Fermions in Loop Quantum Cosmology and the Role of Parity" http://arxiv.org/abs/0806.2821; onghong Hu, Zhongzhu Liu, Qing Xu, Jun Luo, "Parity-violating macroscopic force between chiral molecules and source mass" http://arxiv.org/abs/0805.1294.

[6] Laurence D. Barron, "Optical activity and time reversal", J. Mol. Phys. **43,** 1395 (1981).

[7] J. Jerphagnon, D. S. Chemla, "Optical activity of crystals", J. Chem. Phys. **65**(4), 1522 (1976); A. M. Glazer, K. Stadnicka, "On the origin of optical activity in crystal structures", J. Appl. Cryst. **19**, 108 (1986).

[8]T. Daniel Crawford, Mary C. Tam, Micah L. Abrams, "The Current State of Ab Initio Calculations of Optical Rotation and Electronic Circular Dichroism Spectra", J. Phys. Chem. A **111**(48), 12057 (2007); Kenneth Wiberg, Yi-Gui Wang, Shaun Wilson, Patrick Vaccaro, James Cheeseman, "Sum-over-States Calculation of the Specific Rotations of Some Substituted Oxiranes, Chloropropionitrile, Ethane, and Norbornenone", J. Phys. Chem. A **110**(51), 13995 (2006).

[9] J. Etxebarria, C. L. Folcia, and J. Ortega, "Origin of the optical activity of silver thiogallate," Appl. Cryst. **33,** 126 (2000).

[10] G. Szivessey and C. Münster, "Über die Prüfung der Gitteroptik bei aktiven Kristallen," Ann. Phys. (Leipzig) **20,** 703 (1934).

[11] Clifford M. Will, "The Confrontation between General Relativity and Experiment", http://arxiv.org/abs/gr-qc/0510072v2

[12] S. Schlamminger, K.-Y. Choi, T. A. Wagner, J. H. Gundlach, and E. G. Adelberger, "Test of the Equivalence Principle Using a Rotating Torsion Balance", Phys. Rev. Lett. **100**, 041101 (2008).

[13] P. G. Mezey, "Rules on chiral and achiral molecular transformations", J. Math. Chem. **17,** 185 (1995).

[14] Michel Petitjean, “On the root mean square quantitative chirality and quantitative symmetry measures”, J. Math. Phys. **40,** 4587 (1999); “Chirality and symmetry measures: A transdisciplinary review”, Entropy **5,** 271 (2003).
[15] Personal communication, Prof. Penelope Smith, Mathematics Dept., Lehigh University.
[16] Howard D. Flack, "Chiral and achiral crystal structures", Helv. Chim. Acta **86**, 905 (2003)
[17] Michel Petitjean, J. Math. Phys. **43**, 4147 (2002).
[18] K. Kihara, “An X-ray study of the temperature dependence of the quartz structure”, Eur. J. Mineralogy **2,** 63 (1990).
[19] A. F. Wright and M. S. Lehmann,,"The structure of quartz at 25 and 590 degrees C determined by neutron diffraction", J. Solid State Chem. **36,** 371 (1981).
[20] M. More, G. Odou, J. Lefebvre, “Structure Determination of Benzil in its Two Phases”, Acta Cryst. B**43**, 398 (1987).
[21] Riley Newman, “Prospects for terrestrial equivalence principle tests with a cryogenic torsion pendulum,” Class. Quantum Grav. **18,** 2407 (2001).
[22] R. Bruce King, Mircea V. Diudea, “The chirality of icosahedral fullerenes” J. Math. Chem. **39**, 596 (2006)
[23] A. Rassat, “Chirality and Symmetry Aspects of Spheroarenes, Including Fullerenes” Chirality **13**, 395 (2001)